Flood Damage Assessment Geospatial Application Using Geoinformatics and Deep Learning Classification

https://doi.org/10.3991/ijim.v16i21.34281

Supattra Puttinaovarat[1](✉), Aekarat Saeliw[1], Siwipa Pruitikanee[1], Jinda Kongcharoen[1], Supaporn Chai-Arayalert[1], Kanit Khaimook[2]
[1] Prince of Songkla University, Surat Thani, Thailand
[2] Ramkhamhaeng University, Bangkok, Thailand
supattra.p@psu.ac.th

Abstract—The data of impacts and damage caused by floods is necessary for manipulation to assist and relieve those impacts in each area. The main issue for data acquisition was acquisition methods that affect the durations, accuracy, and completeness of data obtained. Most data are currently obtained by field survey for data on impacts in each area. However, this method contains limitations, i.e., taking a long time, high cost, and no real-time data visualization. Thus, this research presented the study to develop an application for inspecting areas under impact and damage caused by floods using deep learning classification for flood classification and land use type classification in the affected areas using digital images, remote sensing data, and crowdsource data notified by users through the accuracy assessment application of classification. It was found that deep learning classification for flood classification had 97.50% accuracy, with Kappa = 0.95. Land use type classification had 93.72% accuracy, with Kappa = 0.91. Flood damage assessment process in this research was different from other previous research that used geospatial data for flood damage inspection. In previous research, there was no platform to provide users with information about the impact and damage caused by floods in each area. Also, the data cannot be visualized in real-time. In contrast, this research brought damage data notified by users for processing with flood data in each area by satellite image processing and land use types of classification. The proposed application can calculate damage in each area and visualize real-time results in maps and graphs on the dashboard via the application. Besides, the presented method can be used to verify and visualize data of areas under impact and damage caused by floods in different areas.

Keywords—flood damage assessment, geoinformatics, deep learning classification

1 Introduction

Floods are one of most frequent disasters, and cause impacts as well as damage in different areas depending on land use and land cover type (LULC types) in flooded areas [1-3]. According to the studies on the statistics of floods in Thailand during the past 10 years, it was found that floods have occurred every year, with the different

severe levels of floods in each area of each year [4-6]. Most assessment of impacts and damage caused by floods currently relies on field survey by manpower [7-9] to verify and record data to report to government agencies for remedy and assistance of victims from different groups. There are several limitations of field survey, i.e., taking a long time that causes delay of data acquisition of impacts and damage in each area, and high cost due to many surveyors required. Apart from field survey, current advance in geoinformatics, i.e., remote sensing (RS), global positioning system (GPS), and geographic information system (GIS) facilitate the use of satellite images for flooded area inspection using digital image processing [6][8-18]. Thus, this technology helps inspecting which areas contain or do not contain floods. It can also inspect which areas are affected by floods [19-29]. However, there is a limitation of inspection using satellite image processing, i.e., the levels of impacts or damage in each area cannot be inspected, including other related details, e.g., damaged types of area and involved victims.

Moreover, for inspection using satellite image processing, low or middle resolution satellite images cannot specify areas under impacts or damage in spatial details [8][30-32], e.g., whether or not houses or residences are affected. That is because they cannot be seen through satellite images. Also, impacts of floods do not cause damage as much as in some cases. For example, although some plants can endure floods, they are still affected anyway as they cannot be harvested. In contrast, some other plants undergoing damage or dying of floods receive higher-value impacts. This include some endurable plants that cannot be harvested, e.g., oil-palm plantation or rubber plantation [33-35]. It implies that using only satellite images cannot inspect impacts and damage. In addition, most of the current geospatial platforms related to flood management are capable of some aspects such as flood forecasting, flood situation assessment, and flood classification. However, there is still a lack of a platform to monitor the impact and damage caused by floods using crowdsourcing data and remote sensing data that supports real-time processing and visualization. Thus, this research presented the development of a spatial web application to be notified of areas under impacts or damage caused by floods using GIS, GPS, and RS. What's more, the developed web application could bring the data notified by victims to verify with the data in LULC map and flood map obtained using satellite image processing for specifying related data, i.e., affected area types (LULC types) and floods during the time of data notification in each area. This research used deep learning classification to examine and screen data of flood-affected areas and land use types using digital photographs. However, using deep learning classification to identify flood-affected areas requires various costs, including hardware, Random Access Memory (RAM), high-speed broadband internet and Graphics Processing Unit (GPU). This requires a high initial investment, but the advantage is that it is a one-time investment but can be used to monitor and display real-time data. Nonetheless, if traditional field surveys are used to monitor flood-affected areas, a cost is required every time a flood occurs.

2 Related work

2.1 Flood damage assessment

According to the review of literatures and research related to assessment of impacts and damage caused by floods using GIS and RS, it was found that there were 3 types of research, i.e., flooded area inspection [6][8-18], inspection and assessment of damage caused by floods [19-21][23-28], and the development of applications to inspect and assess damage caused by floods [23][29]; to be described in details as follows. According to research on flooded area inspection, it was found that Puttinaovarat et al. (2015) presented the inspection method using satellite image processing by Landsat 8 and MODIS. Different techniques to analyze normalized difference index were used, along with multivariate mutual information, and data fusion by majority voting and Dempster-Shafer. According to the results of their study, it was found that flood area inspection was with 90% accuracy [8]. The results were congruent with another related research. To clarify, it was found that flooded area inspection using satellite image processing could inspect flooded areas. For the limitations of the research, damage in each area could not be specified. Flood damage value could not be visualized.

According to the related research on inspection and assessment of damage caused by floods, it was found that Sajjad et al. (2017) presented an inspection and assessment of damage caused by floods in Pakistan using satellite image processing by Landsat 8 for finding flooded areas and LULC classification. The inspection analyzed modified normalized difference water index (MNDWI). LULC classification used maximum likelihood classification. The results revealed that the number of damaged areas caused by floods was visualized in 2 types, i.e., built-up area and agricultural area. For the limitation of the research, the primary damage value in each area could not be assessed. [21] Prütz and Månsson (2021) presented the method to inspect impacts and damage caused by floods using flood simulation in each area by HEC-RAS Model. The results were brought to analyze impacts and damage using LULC data. The analysis results revealed types of areas under impacts and damage, e.g., agriculture area, commercial area, industrial area, and residential area. For the limitation of the research, if the simulation results were inaccurate, the analyzed data of impacts would also contain errors [19].

Arun and Premalatha (2020) presented the review of literatures and research related to damage caused by floods using remote sensing and GIS. According to the study, it was found that the different types of remote sensing data, i.e., satellite image, LULC data, and digital elevation model (DEM) were used to inspect the affected areas. All methods in previous research still contained a limitation, i.e., no online platform to inspect damage or impacts caused by floods that could analyze, manipulate, and visualize real-time data [20]. Pastor et al. (2018) presented the method to inspect the affected areas using satellite image processing to visualize the results of those affected areas, compared with the map of density of the population in each area. Furthermore, big data from social media was also presented, e.g., the posted number of the victims from Twitter was visualized. For the limitation of the research, lack of data manipulation platform

made it impossible to report the results of the affected areas immediately for involved persons [24].

Van et al. (2019) presented a tool to inspect impacts of floods using LULC map and socio-economic data to for damage mapping, along with analysis of the flooded areas using the data of digital elevation model, hydraulic model, and hydrologic model. The development of the tools used Python programming language. The database system used PostgreSQL and PostGIS. For the limitation of the research, no data from the victims had been used to assess impacts before. Thus, the data of floods might not be incomplete and rough, e.g., types of land use in the affected area. Impacts depended on types of land use, e.g., residences, oil palm farms, orchards, and the business sector, which were affected differently [23]. Glas et al. (2017) presented assessment of damage caused by floods using GIS to analyze LULC data, economic data, flood hazard map, and the data of population. The analysis result was the map of the damaged areas caused by floods, classified by types of areas, i.e., built-up area and rural area; and classified by the levels of damage. For the limitation of the research, the real-time data could neither be analyzed nor visualized. Manpower was required to search for data or to verify data from the static map in case users would like to acknowledge the data of damage at the village level or the expected coordinates [28].

Glas et al. (2016) presented assessment of damage caused by floods using GIS by LULC data, road data, building data, and crop data. Flood map was used to analyze for assessing damage in the 3 types of areas (Road, building, and crop). This made users acknowledge types of the affected areas and could assess damage value. For the limitation of the research, the map used was the static map. Thus, the real-time data could not be visualized [25]. Memon et al. (2015) presented the method to inspect damage in the affected areas using satellite image processing in Pakistan. To clarify, MODIS images were processed to find the flooded areas and to specify the damaged areas. LULC data was also used to specify types of areas under damage. For the limitation of the research, GIS Packaging Software was used for data analysis, which was limited by no real-time data to be visualized for involved persons [26]. Haq et al. (2012) presented the method to inspect the flooded areas and to assess damage using normalized difference water index (NDWI) and water levels for analysis and flood mapping by MODIS and Landsat 7. This could specify the flooded areas and the damaged areas caused by flood [27].

In Thailand, there is the development of flood monitoring system using data of Geo-Informatics and Space Technology Development Agency (Public Organization) (GISTDA). The system is basically related to inspection of impacts and damage in flooded areas using satellite images to help analysis and monitoring in expected areas. Users can also simulate flooded areas in each province and prepare the report of each province about areas of recurrent floods. They can even also assess damage in LULC areas, i.e., agricultural area and residential area [29]. According to the review of related literatures and research, it was found that there is current inspection and assessment of damage in flooded areas using satellite images for processing to inspect those areas. Then, images obtained are analyzed to assess damage in flooded areas. The current system cannot analyze damage immediately because satellite images as semi real-time data are required, finally causes delayed data analysis and verification. Also, there has

been no application for the flooded area inspection and damage assessment system to be notified of impacts and damage yet, including to be verified with related data for analysis and for real-time data visualization.

2.2 Flood susceptibility analysis using machine learning

According to literature review and research on flood susceptibility analysis using machine learning (ML) and spatial data analysis, it was found that flood vulnerability assessment of watershed was presented using analytical network process and fuzzy theories. Therefore, flood vulnerability map could be analyzed into 5 classes, i.e., very high flood, high flood, moderate flood, low flood, and very low flood. According to risk assessment, flood vulnerability map can be used for flood surveillance in each area [36]. However, this research neither presented accuracy of the method nor any platforms or applications for real-time flood inspection in each area. As a result, users could not access changed data in each duration. This research conformed to presentation of flood susceptibility mapping using different ensemble algorithms, i.e., generalized linear model (GLM), flexible discriminate analyses (FDA), multivariate adaptive regression spline (MARS), and random forest (RF). Ensemble algorithms generated more accurate results because the techniques with high accuracy were used for flood susceptibility mapping by voting the result obtained from each technique for flood susceptibility. In this research, the results were classified into 4 classes, i.e., very high flood, high flood, moderate flood, and low flood. The prominence of this research was the results with high accuracy, AUC between 0.89 - 0.94. Flood susceptibility map obtained could be used for flood surveillance in each area [37]. The limitations of this research were the same as the previous research. [36] Also, the limitation of both was that despite flood risk assessment in each area, it did not cover flood impact and damage assessment process in real situation. Therefore, it did not support the operation of flood mitigation, which was necessary for flood management and helping victims. Both researches as aforementioned conformed to the 2 techniques of ML as presented, i.e., fuzzy-value function (FVF) and analytical network process (ANP) for flood susceptibility mapping. This was like this research [36]. However, this also included accuracy assessment. It was found that flood risk analysis or flood susceptibility analysis had 89.1% accuracy. The results could be used for flood surveillance and monitoring [38].

Besides, flood risk analysis was also presented using TOPSIS model and ML algorithms, i.e., random forest (RF), support vector machine (SVM), and boosted regression tree (BRT). The results of risk analysis were classified into 5 classes, i.e., very high flood, high flood, moderate flood, low flood, and very low flood. According to model performance evaluation, it was found that RF was most accurate, followed by SVM and BRT, with AUC of 0.958, 0.899, and 0.865, respectively. Therefore, flood risk map obtained could be used for flood surveillance in each area [39]. There was a study on urban flood-risk assessment using analytic hierarchy process (AHP) and ML algorithms, i.e., classification and regression trees (CART), RF, BRT, MARS, multi-variate discriminant analyses (MDAs), and SVM. Flood risks were classified into 5 classes, i.e., very high flood, high flood, moderate flood, low flood, and very low flood. According to the study results and accuracy assessment of flood risk assessment using ML

algorithms, it was found that CART was most accurate, with 98.50% accuracy in case training dataset was used; and with 89.20% accuracy in case validation dataset was used [40]. Flash flood hazard assessment using ensemble machine learning (EML) algorithms was presented, i.e., generalized linear model by likelihood based (GLMBoost), RF, and Bayesian generalized linear model (BayesGLM). Flash flood map obtained from analysis was classified into 5 classes, i.e., very high flood, high flood, moderate flood, low flood, and very low flood. According to the study results and accuracy assessment, it was found that RF was most accurate, with 92.00% accuracy. GLMBoost and BayesGLM were equally with 90.00% accuracy. However, no accuracy was presented in the research in case EML was used. Therefore, it failed to prove that EML was more accurate than RF for flood risk assessment [41]. Moreover, EML algorithms was also used for flood susceptibility analysis, i.e., MDA, CART, and SVM. Flood susceptibility map in this research was classified into 4 classes, i.e., very high flood, high flood, moderate flood, and low flood. According to accuracy assessment. It was found that EML was most accurate for analysis, with AUC of 0.91. As for using only any one of other algorithms, it was found that MDA, SVM, and CART were with AUC of 0.89, 0.88, and 0.83, respectively. The results of this research proved that using EML for flood susceptibility analysis was more accurate than using one algorithm only [42]. What's more, according to literature review and research on using ML for flood susceptibility analysis, it was found that deep learning algorithm of deep belief network (DBN), a type of ML, was used for flood susceptibility analysis compared with other ML algorithms, i.e., artificial neural network-radial basis function (ANNRBF), logistic regression (LR), logistic model tree (LMTree), functional tree (FTree), an alternating decision tree (ADTree). Flood susceptibility was classified into 5 classes, i.e., very high flood, high flood, moderate flood, low flood, and very low flood. According to algorithm performance evaluation, it was found that DL was most efficient, with AUC of 0.967. Other algorithms, i.e., ANNRBF, ADTree, LMTree, FTree, and LR were with AUC of 0.917, 0.902, 0.892, 0.863, and 0.837, respectively. The evaluation results implied that deep learning generated higher AUC than other algorithms at least by 5%. Therefore, flood susceptibility map obtained could be used for more accurate flood surveillance [43].

According to literature review and related research, it was found that the previous research used ML for flood risk analysis or flood susceptibility analysis. The prominence was that map obtained could be used for flood surveillance in each area to prepare for dealing with upcoming floods. However, that research still contained some limitations. To clarify, they did not cover did not cover flood management in term of flood impact and damage assessment in each area. Therefore, it could not be used in flood mitigation process. In addition, for other previous research with flood damage assessment using geospatial data and ML, several limitations were found. To clarify, flood damage assessment in each area used satellite image processing only, which still contained the limitation in term of loss assessment in each area. More specifically, low, or middle resolution satellite images make it impossible for impact inspection in each area. Furthermore, flood damage assessment in each area using satellite image for LULC types of inspection in affected areas also contained the limitation in term of LULC classification at Level 2 and 3 in case very-high satellite images were not used. For

example, it could not differentiate types of agricultural lands, e.g., oil-palm plantation and rubber plantation. This affected data use for flood damage assessment. Also, ground survey was used in flood damage inspection process in each area. This method caused delay of implementation, finally resulting in assistance and remedies provided to victims in each area. Because of all limitations of the previous research, this research introduced the development of a flood impact and damage inspection application using geoinformatics and deep learning classification. The application can be used during and after floods. Different user groups can manage data of flood impacts and damage in each area. Other than these, our research could reduce the limitations of the previous research because we brought crowdsource data, both attribute data and geospatial data, obtained from notification of victims for data processing with other geospatial data, e.g., flood data and LULC data obtained from satellite image processing. For data processing by the proposed application, it can be processed automatically and supports real-time data visualization.

3 Methodology

The conceptual framework of this research is in Figure 1., consisting of the 4 main parts, i.e., data manipulation, data verification, data visualization of the areas under impacts caused by floods, and using data on Cloud as the input for processing to analyze the areas under impacts and damage caused by floods. The details in each part will be described in section 3.1-3.5. The theories and technologies used in this research included ML technique. To clarify, deep learning was used for digital image classification between the flooded areas and the non-flooded areas. It was also used for image classification of types of land use, i.e., agricultural area, urban area, and others; digital image processing based on remote sensing data for flood classification; GIS; GPS; RS; and IT to develop an application to inspect and to be notified of impacts or damage caused by floods. In addition, the proposed research has a workflow of the geospatial platform shown in Figure 2, which consists of three processes: data querying, data processing, and data visualization using the dashboard.

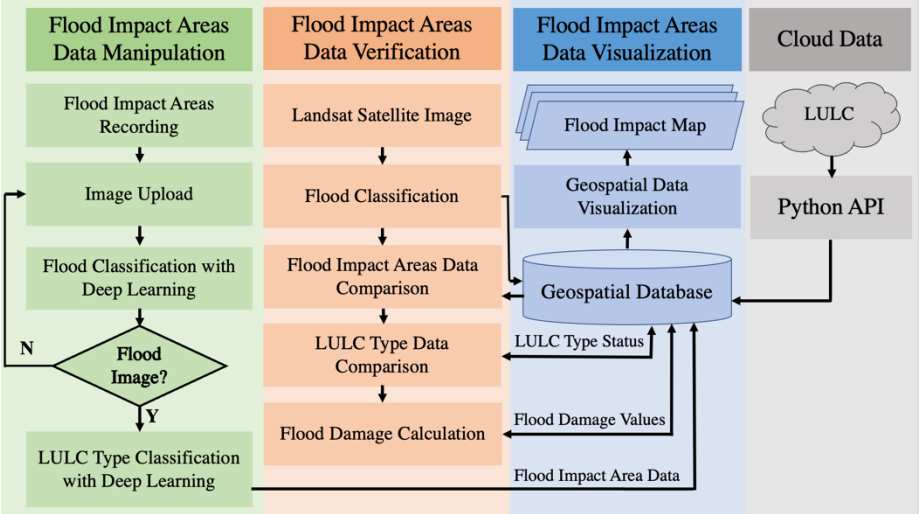

Fig. 1. Purpose conceptual framework

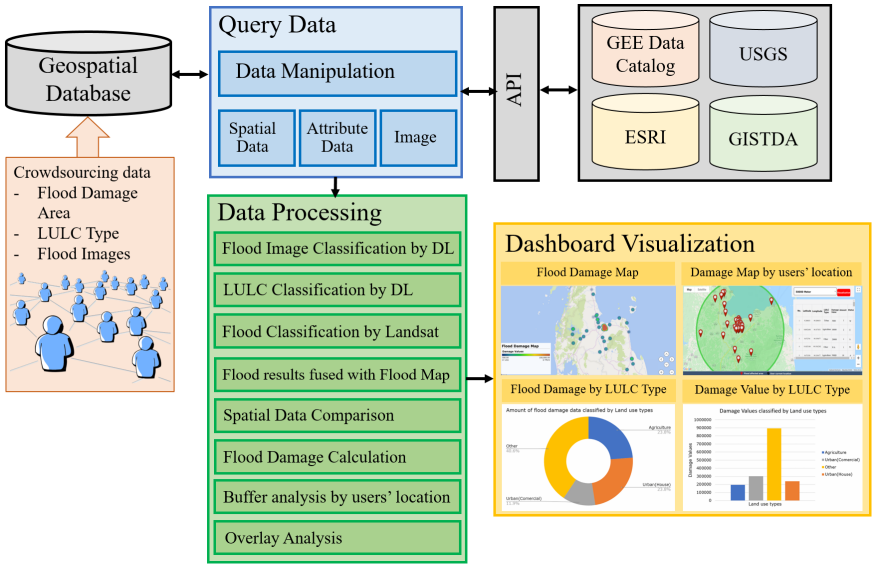

Fig. 2. Workflow of purpose geospatial platform

3.1 Data collection and preparation

This research included attribute and spatial data from different sources for trial and application development, as in Table 1. There were 3 study areas, i.e., Surat Thani Province, part of Chumphon Province, and part of Nakhon Si Thammarat Province in

the upper south of Thailand. These study areas undergo floods nearly every year. Therefore, it is necessary to regularly survey and record the impact and damage caused by floods using a digital platform. There were several platforms for data input, i.e., coding for data input from Cloud, photography, input through keyboards or touchscreen on smartphones, and uploading data in digital platform. These methods could be done through the application presented in this research.

The process of monitoring the impact and damage caused by floods in this study uses medium to high-resolution data. The resolution of the data used in this study is revealed in Table 2. Although the use of medium-resolution data has limited the spatial resolution of the impacts and damage investigations of flooding. However, the data quality can be adjusted by fusing medium-resolution data with high-resolution data. This research combines flooding data from Landsat image processing with a flood map obtained from GISTDA. Flood maps obtained from GISTDA are processed using high-resolution satellite imagery. In addition, the methods for monitoring the impact and damage from floods presented in this research support the change in high-resolution satellite imagery.

Table 1. Data and data sources

Data	Type	Data sources	Period/Frequency
Flood photo	Spatial	Crowdsource	Real-time
Non-Flood photo	Spatial	Crowdsource	Real-time
Flood photo in agriculture area	Spatial	Crowdsource/Survey	Real-time
Flood photo in urban area	Spatial	Crowdsource/Survey	Real-time
Flood photo in other area	Spatial	Crowdsource/Survey	Real-time
Landsat 8	Spatial	USGS	16 Day
LULC	Spatial	ESRI, GEE Data Catalog	2020
Flood map	Spatial	GISTDA	2020
Flood impact area	Spatial Attribute	Crowdsource	2020

Table 2. Data resolution

Data	Image Resolution	Resolution Level
Flood photo	Real situation	High
Non-Flood photo	Real situation	High
Flood photo in agriculture area	Real situation	High
Flood photo in urban area	Real situation	High
Flood photo in other area	Real situation	High
Landsat 8	30 M	Medium
LULC	10 M	Medium
Flood map	2-5 M	High
Flood impact area	Real situation	High

3.2 Data manipulation

This research developed the application to inspect and to be notified of impacts or damage caused by floods. To be notified of impacts or damage, users or victims could send notification through the developed application. The web application could fetch data of current coordinates in terms of latitude and longitude. Users could record attribute data, i.e., types of land use, subtypes of affected areas (Oil-palm plantation, residences, and establishments), damage value, the number of affected areas, and images of affected areas. In the data hiring process in this research, deep learning classification was used for uploaded image classification. If they were the images of flooded areas, users could notify of data. But if they were not, users must upload images again for further notification. Deep learning classification (Convolutional Neural Network) was used for LULC types of classification in digital images, classified into 3 types, i.e., agricultural area, urban area, and others. For the details of modelling using deep learning for flood classification, along with modelling using deep learning for LULC types of classification, as in Table 3 and Figure 3. A hyperparameter optimization was used to determine the appropriate parameters for modeling in this study, as revealed in Figure 4.

Table 3. Deep learning classification parameters

Parameters	Flood classification	LULC types classification
Number of Class	2	3
Image size	224*224	224*224
Batch size	64	64
Activation function	RELU	RELU
Learning rate	0.01	0.01
Momentum	0.9	0.9
Epochs	10	10
Training and testing data	1000	1050
Validation data	150	150

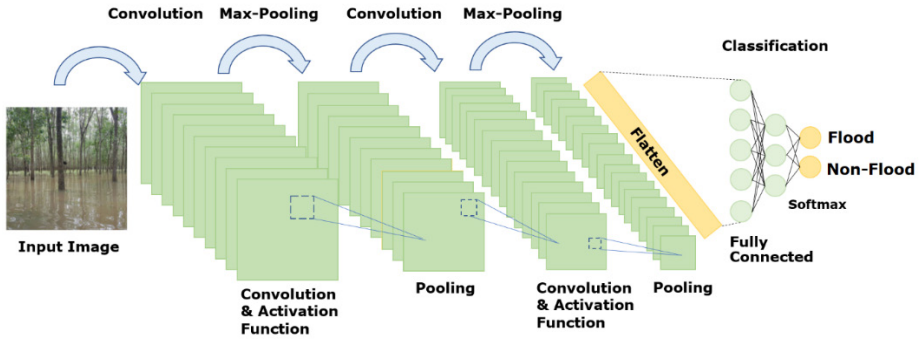

Fig. 3. Purpose deep learning network architecture

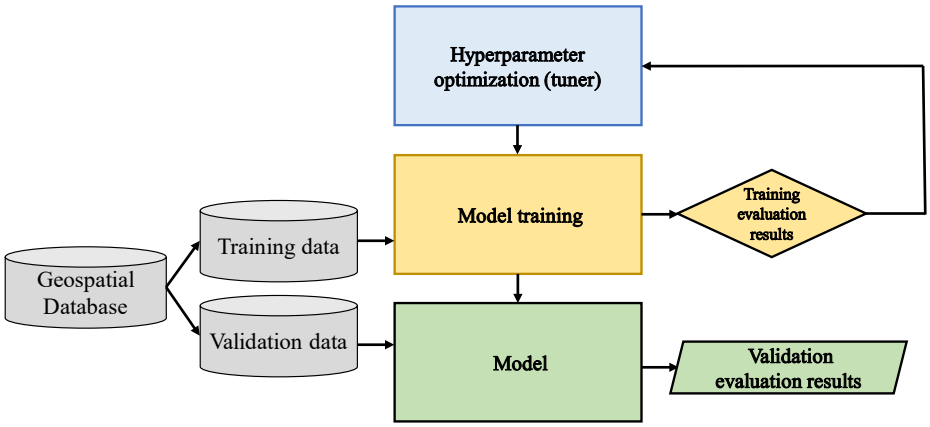

Fig. 4. Purpose method of hyperparameter optimization

3.3 Data verification

For affected area inspection, it included flood classification and comparison of floods notified by users from the data of flood classification. Besides, LULC types were also compared with LULC data to update the status of LULC types whether it matched land use types. The process also included calculation of damages caused by floods, compared with the benchmark. The budget for remedy of damage in each type of area is in Table 4.

Table 4. Thailand' budget for flood mitigation in 2021

Land use type	Budget
Rice	1,340 Baht per Rai
Field crops and vegetables	1,980 Baht per Rai
Fruit trees, perennials, etc.	4,048 Baht per Rai
Residential/House	4,048 Baht per House

3.4 Data visualization

For visualization of the affected data in this research, it was presented in different maps, i.e., online map, satellite map, street map, and cluster marker map. The data was also presented through dashboard. These platforms in the web application presented in this research used computer languages and tools, i.e., PHP, Python, Google Map API, Leaflet, and MySQL for web application development. For spatial data visualization in this research, spatial function was used for spatial data analysis, i.e., geofencing or buffer function to query the affected areas in the determined scope, considered by users' current locations. Overlay function was used to sum or overlay multilayer data, along with logical functions, e.g., AND, OR, and XoR for data processing in decision making in accordance with the conditions.

3.5 Accuracy assessment

Accuracy assessment in this research was divided into 2 parts, i.e., accuracy assessment of digital images for flood classification, and accuracy assessment of LULC types of classification. Assessment of both parts contained parameter calculation, i.e., accuracy, user accuracy, producer accuracy, and Kappa. The data obtained was used for comparison with the classification results from several sources, i.e., digital ground survey, agencies (GISTDA and Department of Land Development of Thailand) and Crowdsource/Volunteered Geographic Information. The calculation equation is in Table 5.

Table 5. Accuracy assessment equations

Method	Expression	Description
Accuracy User's Accuracy Producer's Accuracy	(TP+TN)/(TP+TN+FP+FN) TP/(TP+FP) TP/(TP+FN)	TP (True Positive) TN (True Negative) FP (False Positive) FN (False Negative)
Kappa	[K0-Ke]/[1-Ke]	$Ke = [(TN+FN)\times (FN+FP)+(FP+TP) \times (FN+TP)]/n^2$ K0 = (TN+TP)/n

3.6 System analysis and implementation

For the analysis of system and the developed application in this research, users were divided into 3 groups, i.e., general users, village leaders, and administrators. Users in each group were permitted to use the application with different rights, as per the details of the use case diagram in Figure 5. According to the figure, it was found that general users could notify of the affected areas. But before notification, authentication was required for user identification. Simultaneously, users' current coordinates from GPS in smartphones were also recorded with the data of the affected areas. Other than this, general users could also retrieve the data using geospatial visualization. In this part, users could set the scope of expected areas, e.g., visualization of the affected area within 10 km. from the current location. Village leaders and administrators could use the application like general users but with different rights. To clarify, village leaders could retrieve reports of the affected areas in dashboard and could verify and confirm the data of the affected areas in case of mismatched data. Administrators had the different right to use the application from village leaders. To clarify, administrators could manipulate data of floods obtained by satellite image processing or from uploaded data from involved agencies, e.g., GISTDA to inspect the affected areas notified through the web application.

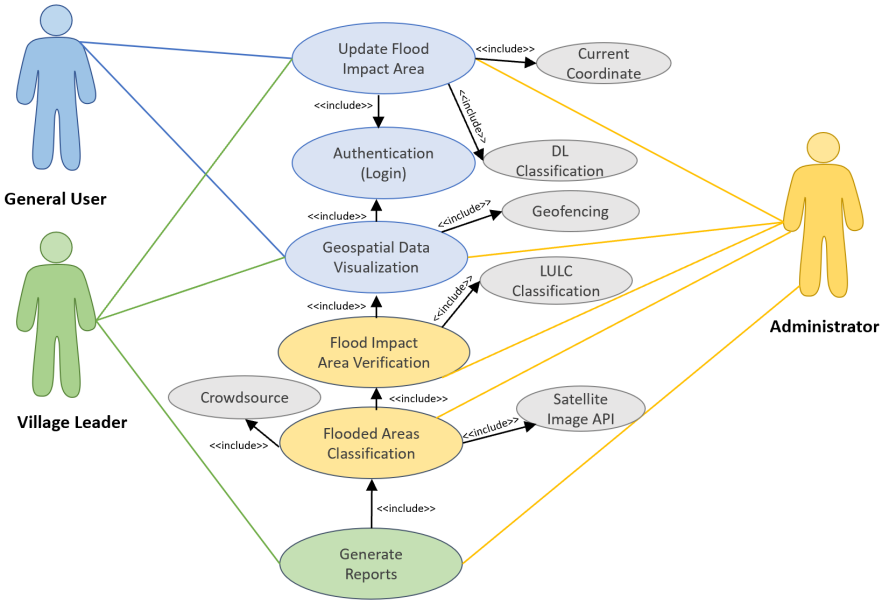

Fig. 5. Use case diagram

4 Results and discussion

The results of this research were divided into 3 parts, i.e., the results of flood classification using deep learning classification, the results of LULC types of classification (Agricultural area, urban area, and others) using deep learning classification, and the results of inspection system development using geoinformatics. The details in each part are as follows.

The results of flood classification using digital images uploaded through the web application. Deep learning technique was used for classification, as in Figure 6. It was found that in case users uploaded digital images of the flooded areas, the results revealed the probabilities of flood class. The research used in the benchmark was that if the probabilities in a class was over 0.5 or 50%, the result obtained would be that class. According to Figure 6(a), it was found that the classification result came out as "Flood," with the probability of 0.98. As for Figure 6(b), the classification result came out as "Non-Flood," with the probability of 1.00. According to visual inspection, it was found that the result of classification of Figure 6(a) and 6(b) was accurate and congruent with the images. However, to prove the accuracy of flood classification method in this research, accuracy assessment of flood classification was used. There were 2 parts of accuracy assessment as follows. The first one was accuracy assessment of 1000 images used as training data, classified as 500 images of flooded areas and 500 images of non-flooded areas. 10-fold cross-validation was used. The second one was accuracy assessment of 100 images, classified as 50 images of flooded areas and non-flooded areas to

compare accuracy of both cases. According to the results, 97.50% classification accuracy was found, with Kappa of 0.95, as in Table 6. When considering the details of classification accuracy in both cases as in Figure 7(a) and 7(b), it was found that the presented technique used in the first case tested with 1,000 images could inspect the flooded areas accurately, with true positive (TP) and true negative (TN) of 48.50 % and 49.00%, respectively. And according to the verification of classification errors, it was found that false positive (FP) and false negative (FN) were 1.50% and 1.00%, respectively. In this research, TP was referred to "Flood," and "Flood" was found indeed according to the inspection. TN was referred to "Non-Flood," and "Non-Flood" was found indeed according to the inspection. FP was referred to "Flood," but "Non-Flood" was found according to the inspection. FN was referred to "Non-Flood," but "Flood" was found according to the inspection. For the results of TP, TN, FP, and FN of all 1,000 images and the results of testing the other 100 images, it was found that they were congruent (As in Figure 7(b)).

Table 6. Flood classification assessment

Data	Class	Accuracy	User's Accuracy	Producer's Accuracy	Kappa
Training and testing data	Flood Non-Flood	97.50	97.98 97.03	97.00 98.00	0.95
Validation data	Flood Non-Flood	96.50	96.97 96.04	96.00 97.00	0.93

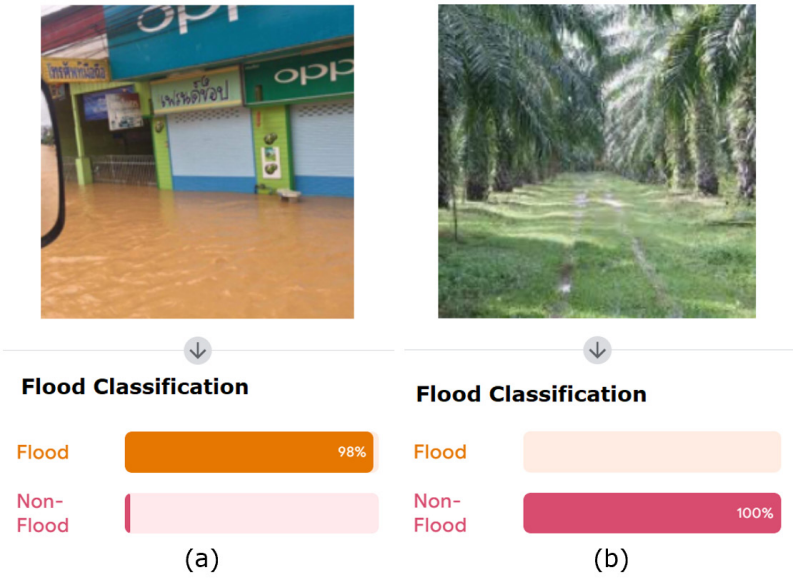

Fig. 6. Flood classification results (a) Flood class (b) Non-Flood class

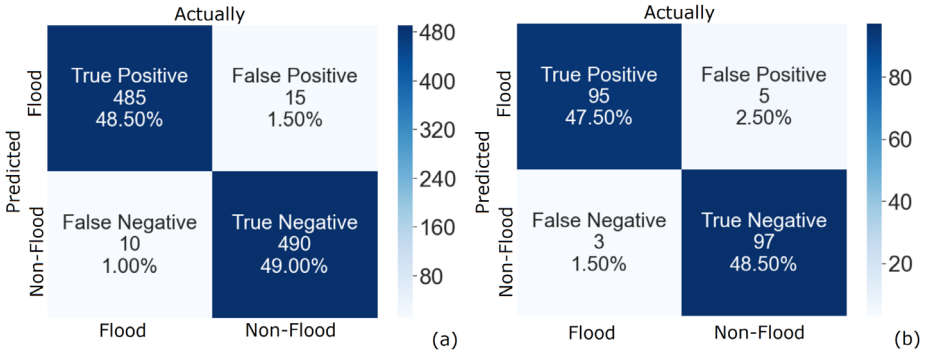

Fig. 7. Confusion matrix of flood classification (a) Training and testing data (b) Validation data

For the results of LULC types of classification using 3 classes of digital images, i.e., agricultural area, urban area, and others using deep learning classification as Figure 8., visualizing the results of classification of digital images in the different classes, i.e., agricultural area, urban area, and others in online map. According to the figure, it was found that classification of each class was 100%. And to verify accuracy classification of each class in the developed web application, the results could be visualized in Google Satellite Map and Google Street Map as in Figure 9(a) - 9(c). According to Figure 9(a), it was found that the uploaded image was an oil palm farm, classified as an agricultural area. This was congruent with the results obtained from classification. As for Figure 9(b), it was found that the uploaded image was classified as "Others." And according to the visualized results of Google Satellite Map and Google Street Map, it was a road. This means the results of classification and the actual area were congruent. And according to Figure 9(c), it was found that the uploaded image was classified as an urban area. And according to the visualized results of Google Satellite Map and Google Street Map, it was a building, classified as an urban area, too.

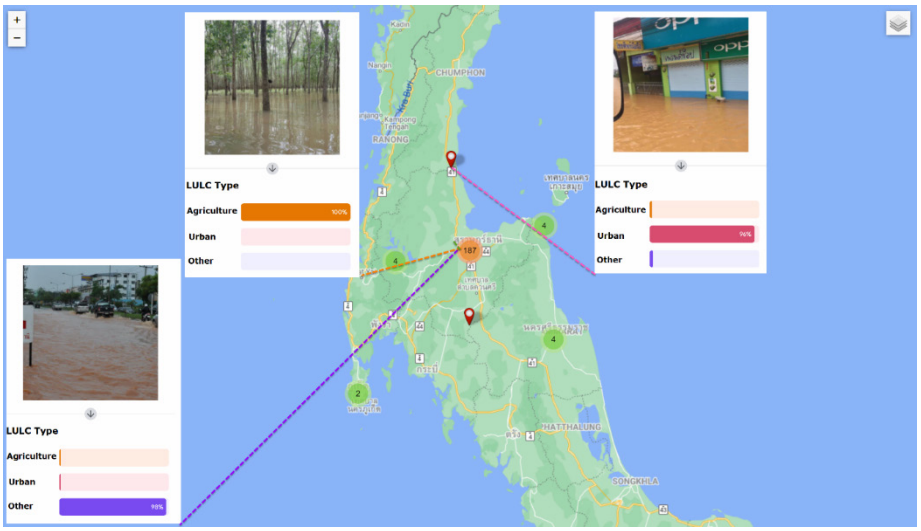

Fig. 8. LULC types classification map using deep learning

In this research, accuracy assessment of LULC types classification was divided into 2 parts. The first part was accuracy assessment of training data and testing data of 1,050 images, i.e., 350 images of agricultural area, 350 images of urban area, and 350 images of other areas. 10-fold cross-validation was used. The second part included 150 images for accuracy assessment of validation data, i.e., 50 images of agricultural area, 50 images of urban area, and 50 images of other areas. According to accuracy assessment in the first part, 93.72% accuracy was found, with Kappa of 0.91. When analyzing accuracy in the details of accurate classification and classification errors in each class, it was found that classification accuracy was equally high in all 3 classes, as in Figure 10(a). For the assessment results in the second part, 92.00% accuracy was found, with Kappa of 0.88. When analyzing accuracy in the details of accurate classification and classification errors in each class, it was found that classification accuracy was equally high in all 3 classes like training data and testing data, as in Fig.10(b). The details of assessment results are in Table 7.

Fig. 9. Land use types classification (a) Agriculture (b) Other (c) Urban

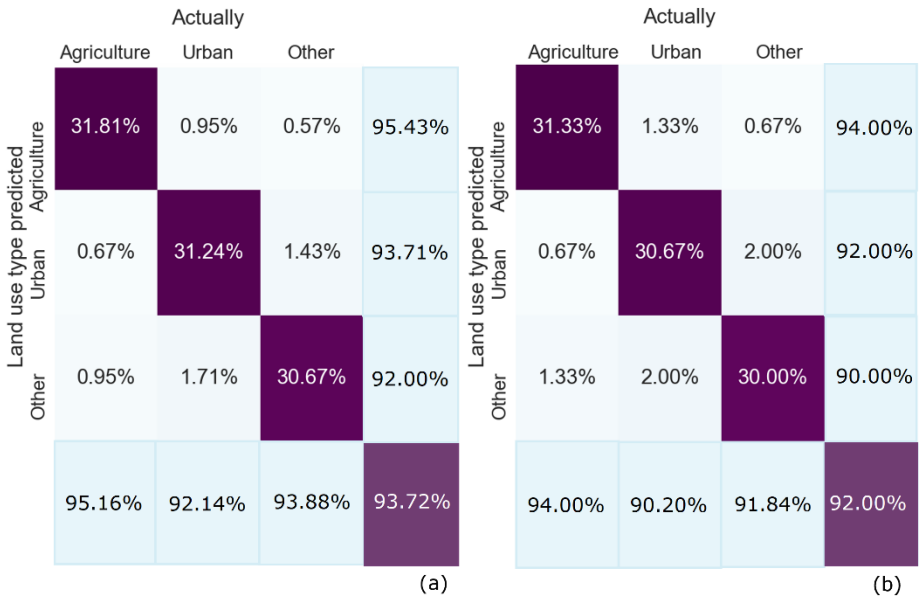

Fig. 10. Confusion matrix of LULC types classification (a) Training and testing data (b) Validation data

Table 7. Flood Classification assessment

Data	Class	Accuracy	User's Accuracy	Producer's Accuracy	Kappa
Training and testing data	Agriculture Urban Other	93.72	95.16 92.14 93.88	95.43 93.71 92.00	0.91
Validation data	Agriculture Urban Other	92.00	94.00 90.20 91.84	94.00 92.00 90.00	0.88

For the results of the inspection system development in this research, they were divided into 3 parts, i.e., the results of system development to be notified of the areas under impacts and damage caused by floods; the results of system development for visualization of the areas under impacts and damage caused by floods based on users' current locations; and the results of system development for inspection, visualization, and report of the areas under impacts and damage caused by floods; including visualization in dashboard to present related data. The results of system development in each part contained the details as follows. The results of system development to be notified of the areas under impacts and damage were visualized in Figure 11(a) and 11(b). According Figure 11(a), it referred to user interface for data notification. Data input included user's current locations (Latitude and longitude), LULC types, LULC detail, damage value, the number of affected areas, and images. Data of latitude and longitude was fetched from GPS in users' smartphones. When data was recorded, the results

would be visualized in Figure 11(b). According to the figure visualizing the affected areas as per notification, the red marker referred to the affected area.

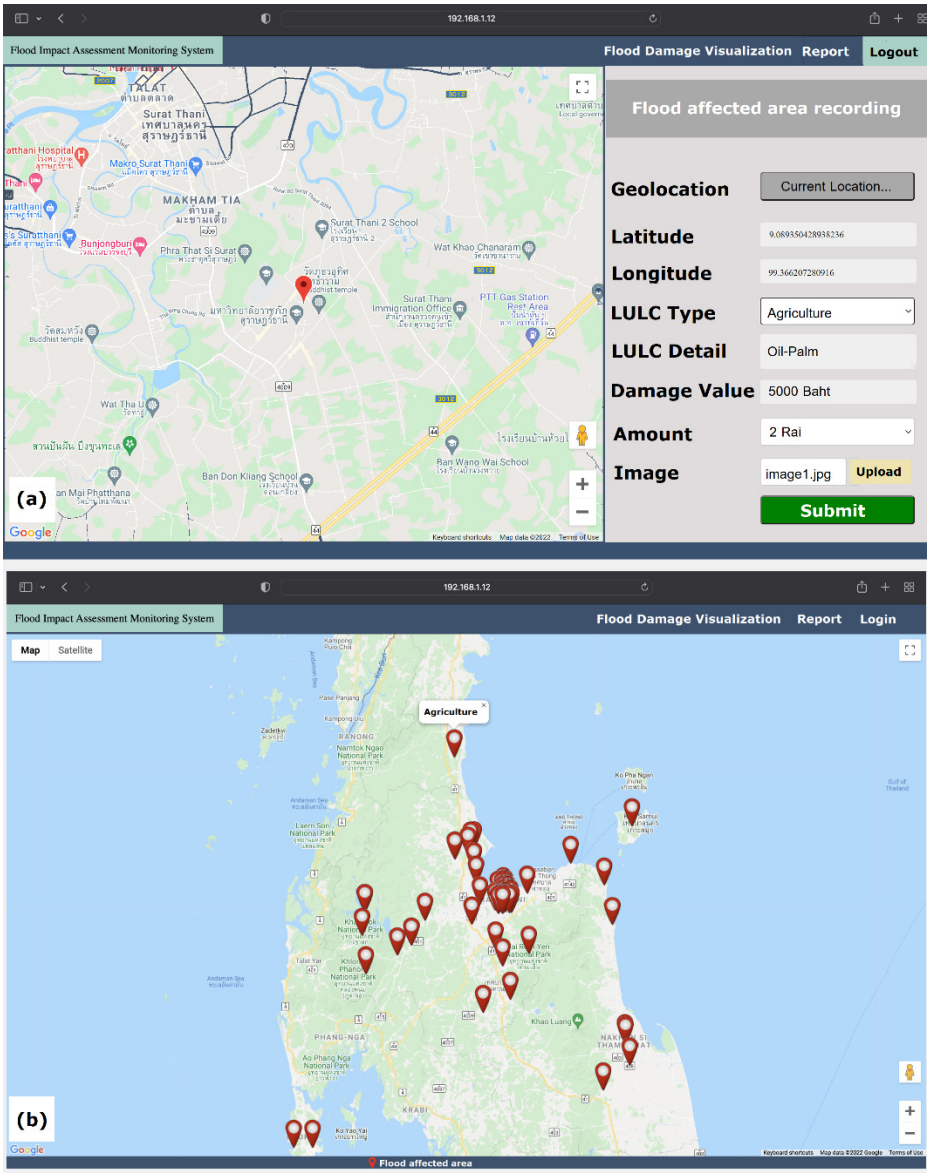

Fig. 11. Web application user interface (a) Input form (b) Visualization of flood affected areas

The results of system development for visualization of the areas under impacts and damage based on users' current locations are in Figure 12(a) - 12(c), with 2 functions, i.e., markers and attribute data in details to describe each marker about each affected

area and the data of inspected impacts in each area. Figure 12(a) visualized the affected area within the scope of 500 meters from user's current location. According to the figure, no affected areas were found within 500 meters. Figure 12(b) visualized the affected area within the scope of 5,000 meters. According to the figure, it was found that markers were inserted in the circle, with the table of attribute data, visualizing the affected areas. Figure 12(c) visualized the affected area within the scope of 50,000 meters from user's current location. Spatial visualization facilitates involved agencies and system users to apply data for further planning and decision making on budget planning as well as allocation to help in each area.

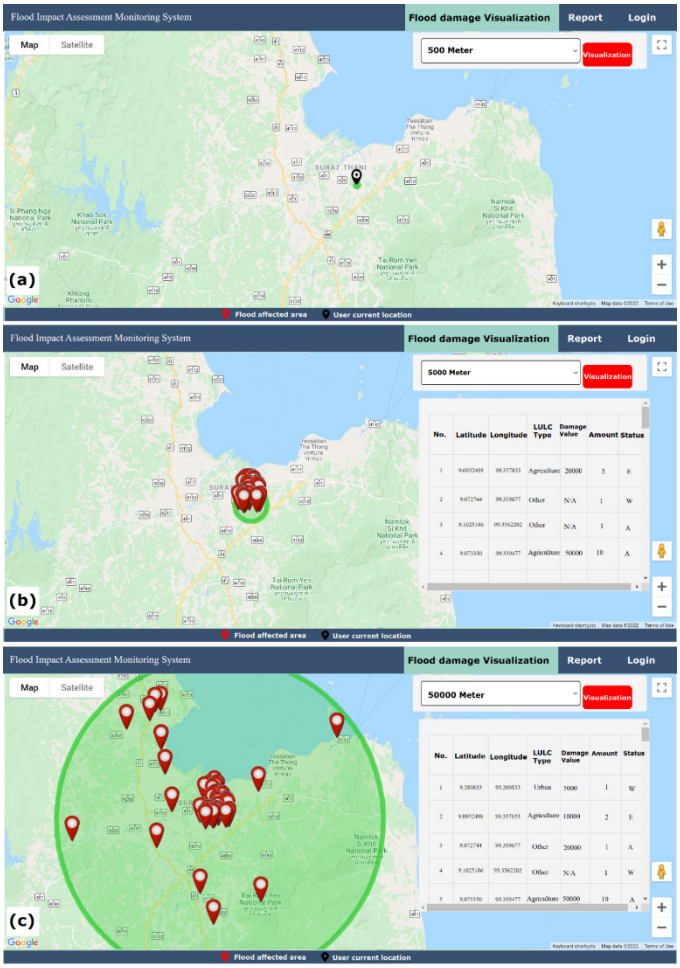

Fig. 12. Flood damage based on users' current locations (a) 500 Meters (b) 5,000 Meters (c) 50,000 Meters

The results of visualization system development for the notified areas were compared with the actual data in each affected area, obtained from involved agencies, e.g.,

GISTDA; along with the data of floods using satellite image processing, as in Figure 13(a) and 13(b). The results of this part were used in village leaders and administrator as supporting data to inspect the affected area, and to be suggested to government agencies for proper and sufficient budget allocation in each affected area. Figure 13(a) visualized the affected areas under flood overlay and the data of floods using satellite image processing. The red markers referred to the affected area whereas the blue polygons referred to the affected area using satellite image processing. Figure 13(b) visualized the affected areas cluster marker map and satellite map that facilitated the overall visualization of largely and slightly affected areas, considered by colored circles in the caps. For example, green referred to there were less than 10 affected areas. Yellow referred to there were over 10 affected areas. Thus, these data could be concluded for quick planning and decision making. Also, the system to query LULC data from ESRI was also developed, using Python API as data for processing to compare land use types obtained from digital image classification. Those images were uploaded by users to find out whether not there were any matched LULC types. This brought auto-inspection with no need to use manpower in case of matched LULC types. But in case of mismatch, village leaders could inspect and confirm the data through the presented system in this research, as in Figure 14.

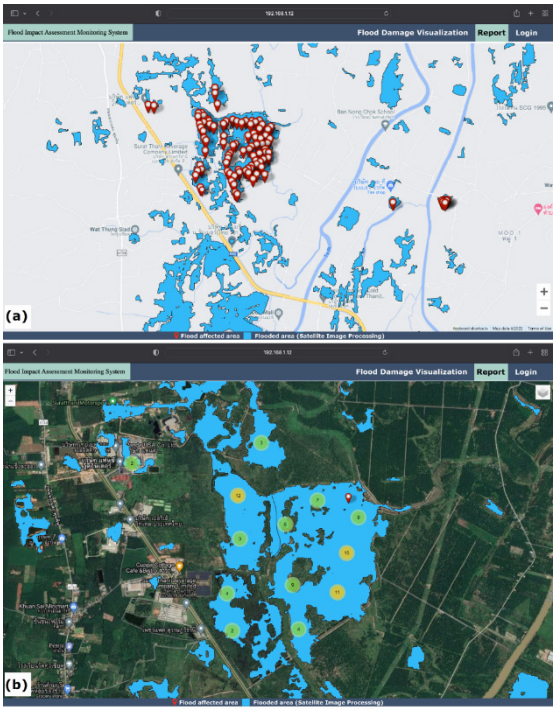

Fig. 13. Flood affected areas map (a) flood affected areas overlay with flood areas using satellite image processing (b) flood affected areas cluster marker map and satellite map

Fig. 14. Flooded areas overlay with ESRI LULC

In this research, the system was developed for visualization of the affected areas in dashboard, i.e., maps, diagrams, graphs, and tables to make it easy for data memorization to support planning and decision making on helping and mitigation of floods in each area, as in Figure 15. According to the figure, the data in map visualizing the affected areas and damages caused by floods in each area, the graph visualizing the amount of data of the affected areas classified by land use types, and the graph visualizing damages classified by LULC types. Real-time dashboard facilitated users to use data for decision making more quickly and more efficiently.

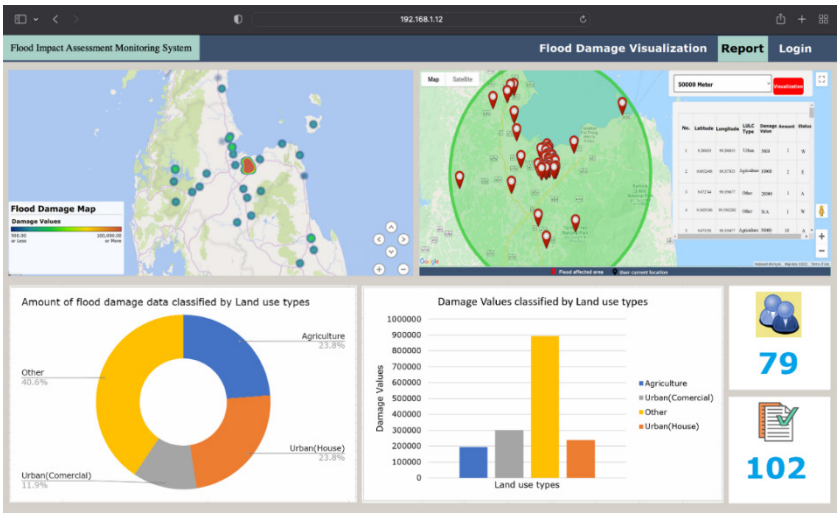

Fig. 15. Dashboard on web application

This research presented the development of data verification application to inspect the areas under impacts and damage caused by flood using deep learning classification and geoinformatics so that different groups of users, i.e., general users, village leaders, and administrators can use the application for manipulation and spatial visualization of the affected areas. According to the results of accuracy assessment of flood classification, 97.50% accuracy was found, with Kappa of 0.95. According to the results of accuracy assessment of LULC types classification using digital images, 93.72% accuracy was found, with Kappa of 0.91. The results of both parts contained high accuracy, and thus they could be used in the application to inspect impacts and damage caused by floods in each area quickly and efficiently.

The previous research contained a number of limitations of inspecting impacts and damage caused by floods, i.e., no application or platform for real-time manipulation [20][24-25][28], no data of LULC in details [23], and incapable application to support users for their notification of affected areas [29]. In this research, the application to inspect impacts and damage caused by floods was developed, along with fixing those limitations as aforementioned. Thus, it can be used for management indeed to help and mitigate floods in each area. Involved government agencies can also use it to support decision making of involved personnel.

5 Conclusion

According to the results of inspection system development for impacts and damage caused by floods using deep learning classification to differentiate and inspect digital images in the flooded and non-flooded areas, along with classification of all 3 land use types, i.e., agricultural area, urban area, and others, it was found that deep learning classification for to differentiate both parts contained high accuracy. This research introduced the development of the flood impact and damage inspection application using geoinformatics and deep learning classification, with contribution in the following issues.

1. Reliability: Bringing data of flood impacts and damage obtained from crowdsource data for further processing by deep learning classification and comparing with flood data and LULC data obtained from satellite image processing generated accurate results that conformed to actual flood damage in each area. The results can be used to support decision-making and planning for fast assistance and remedies to victims in each area.
2. Timeliness: The development of the flood impact and damage inspection application that supports data management and real-time geospatial data display facilitates data and information obtained to be used in time of flood management during and after floods. Its prototype can be applied to other disasters as well.

6 Acknowledgment

The authors would like to thank the Google, USGS, ESRI, GISTDA and the Department of Land Development in Thailand for providing the remotely sensed data used in preparation of the paper. This work was supported by the Faculty of Science and Industrial Technology, Prince of Songkla University, Surat Thani Campus.

7 References

[1] Phinyoyang, A., & Ongsomwang, S. (2021). Optimizing Land Use and Land Cover Allocation for Flood Mitigation Using Land Use Change and Hydrological Models with Goal Programming, Chaiyaphum, Thailand. *Land*, 10(12), 1317. https://doi.org/10.3390/land10121317

[2] Setiyawati, N., Purnomo, H. D., & Mailoa, E. (2022). User Experience Design on Visualization of Mobile-Based Land Monitoring System Using a User-Centered Design Approach. *International Journal of Interactive Mobile Technologies*, 16(3), 47-65. https://doi.org/10.3991/ijim.v16i03.28499

[3] Igarashi, K., Koichiro, K., Tanaka, N., & Aranyabhaga, N. (2019). Prediction of the impact of climate change and land use change on flood discharge in the Song Khwae District, Nan Province, Thailand. *Journal of Climate Change*, 5(1), 1-8. https://doi.org/10.3233/jcc190001

[4] Puttinaovarat, S., & Horkaew, P. (2019). Application Programming Interface for Flood Forecasting from Geospatial Big Data and Crowdsourcing Data. *International Journal of Interactive Mobile Technologies*, 13(11) ,137-156. https://doi.org/10.3991/ijim.v13i11.11237

[5] Prabnakorn, S., Suryadi, F. X., Chongwilaikasem, J., & De Fraiture, C. (2019). Development of an integrated flood hazard assessment model for a complex river system: a case study of the Mun River Basin, Thailand. *Modeling Earth Systems and Environment*, 5(4), 1265-1281. https://doi.org/10.1007/s40808-019-00634-7

[6] Puttinaovarat, S., Horkaew, P., Khaimook, K., & Polnigongit, W. (2015). Adaptive hydrological flow field modeling based on water body extraction and surface information. *Journal of Applied Remote Sensing*, 9(1), 095041. https://doi.org/10.1117/1.jrs.9.095041

[7] Omar, M., Nawi, M. M., Jamil, J., Mohamad, A., & Kamaruddin, S. (2020). Research design of mobile based decision support for early flood warning system. *International Journal of Interactive Mobile Technologies*, 14(17) ,130-140. https://doi.org/10.3991/ijim.v14i17.16557

[8] Puttinaovarat, S., & Horkaew, P. (2020). Internetworking flood disaster mitigation system based on remote sensing and mobile GIS. *Geomatics, Natural Hazards and Risk*, 11(1), 1886-1911. https://doi.org/10.1080/19475705.2020.1815869

[9] Horkaew, P., Puttinaovarat, S., & Khaimook, K. (2015). River Boundary Delineation From Remotely Sensed Imagery Based On SVM And Relaxation Labeling Of Water Index And DSM. *Journal of Theoretical & Applied Information Technology*, 71(3), 376-386.

[10] Seydi, S. T., Saeidi, V., Kalantar, B., Ueda, N., van Genderen, J. L., Maskouni, F. H., & Aria, F. A. (2022). Fusion of the Multisource Datasets for Flood Extent Mapping Based on Ensemble Convolutional Neural Network (CNN) Model. *Journal of Sensors*, 2022. https://doi.org/10.1155/2022/2887502

[11] Farhadi, H., Esmaeily, A., & Najafzadeh, M. (2022). Flood monitoring by integration of Remote Sensing technique and Multi-Criteria Decision Making method. *Computers & Geosciences*, 160, 105045. https://doi.org/10.1016/j.cageo.2022.105045

[12] Mahmud, H. B., Katiyar, V., & Nagai, M. (2021). Improved consistency of an automated multisatellite method for extracting temporal changes in flood extent. *Mathematical Problems in Engineering*, 2021. https://doi.org/10.1155/2021/6164161

[13] Zhang, L., & Xia, J. (2021). Flood Detection Using Multiple Chinese Satellite Datasets during 2020 China Summer Floods. *Remote Sensing*, 14(1), 51. https://doi.org/10.3390/rs14010051

[14] Kocaman, S., Tavus, B., Nefeslioglu, H. A., Karakas, G., & Gokceoglu, C. (2020). Evaluation of floods and landslides triggered by a meteorological catastrophe (Ordu, Turkey, August 2018) using optical and radar data. *Geofluids*, 2020. https://doi.org/10.1155/2020/8830661

[15] Gao, Y., Liang, Z., Wang, B., Wu, Y., & Wu, P. (2018). Wetland change detection using cross-fused-based and normalized difference index analysis on multitemporal Landsat 8 OLI. *Journal of Sensors*, 2018. https://doi.org/10.1155/2018/8130470

[16] Singh, A., & Singh, K. K. (2017). Satellite image classification using Genetic Algorithm trained radial basis function neural network, application to the detection of flooded areas. *Journal of Visual Communication and Image Representation*, 42, 173-182. https://doi.org/10.1016/j.jvcir.2016.11.017

[17] Ahamed, A., & Bolten, J. D. (2017). A MODIS-based automated flood monitoring system for southeast asia. *International Journal of Applied Earth Observation and Geoinformation*, 61, 104-117. https://doi.org/10.1016/j.jag.2017.05.006

[18] Tong, X., Luo, X., Liu, S., Xie, H., Chao, W., Liu, S., ... & Jiang, Y. (2018). An approach for flood monitoring by the combined use of Landsat 8 optical imagery and COSMO-SkyMed radar imagery. *ISPRS journal of photogrammetry and remote sensing*, 136, 144-153. https://doi.org/10.1016/j.isprsjprs.2017.11.006

[19] Prütz, R., & Månsson, P. (2021). A GIS-based approach to compare economic damages of fluvial flooding in the Neckar River basin under current conditions and future scenarios. *Natural Hazards*, 108(2), 1807-1834. https://doi.org/10.1007/s11069-021-04757-y

[20] Arun, R., & Premalatha, K., Flood Damage Assessment using Remote Sensing and GIS: The Past And Present, (2020). *International Journal of Civil Engineering and Technology (IJCIET)*, 11(12). https://doi.org/10.34218/ijciet.11.12.2020.001

[21] Sajjad, A., Lu, J., Chen, X., Chisenga, C., Saleem, N., & Hassan, H. (2020). Operational monitoring and damage assessment of riverine flood-2014 in the lower Chenab plain, Punjab, Pakistan, using remote sensing and GIS techniques. *Remote Sensing*, 12(4), 714. https://doi.org/10.3390/rs12040714

[22] Psomiadis, E., Soulis, K. X., Zoka, M., & Dercas, N. (2019). Synergistic approach of remote sensing and gis techniques for flash-flood monitoring and damage assessment in Thessaly plain area, Greece. *Water*, 11(3), 448. https://doi.org/10.3390/w11030448

[23] Van Ackere, S., Beullens, J., Vanneuville, W., De Wulf, A., & De Maeyer, P. (2019). FLIAT, An object-relational GIS tool for flood impact assessment in Flanders, Belgium. *Water*, 11(4), 711. https://doi.org/10.3390/w11040711

[24] Pastor-Escuredo, D., Torres, Y., Martinez, M., & Zufiria, P. J. (2018). Floods impact dynamics quantified from big data sources. arXiv preprint arXiv:1804.09129.

[25] Glas, H., Van Ackere, S., & Deruyter, G. (2016). Flood damage assessment in a GIS: Case study for Annotto Bay, Jamaica. *Int. J. Saf. Secur. Eng*, vol. 6, pp. 508–517. https://doi.org/10.2495/safe-v6-n3-508-517/006

[26] Memon, A. A., Muhammad, S., Rahman, S., & Haq, M. (2015). Flood monitoring and damage assessment using water indices: A case study of Pakistan flood-2012. *The Egyptian Journal of Remote Sensing and Space Science*, 18(1), 99-106. https://doi.org/10.1016/j.ejrs.2015.03.003

[27] Haq, M., Akhtar, M., Muhammad, S., Paras, S., & Rahmatullah, J. (2012). Techniques of remote sensing and GIS for flood monitoring and damage assessment: a case study of Sindh province, Pakistan. *The Egyptian Journal of Remote Sensing and Space Science*, 15(2), 135-141. https://doi.org/10.1016/j.ejrs.2012.07.002

[28] Glas, H., Jonckheere, M., Mandal, A., James-Williamson, S., De Maeyer, P., & Deruyter, G. (2017). A GIS-based tool for flood damage assessment and delineation of a methodology for future risk assessment: case study for Annotto Bay, Jamaica. *Natural Hazards*, 88(3), 1867-1891. https://doi.org/10.1007/s11069-017-2920-5

[29] GISTDA (2021). Thailand Flood Monitoring System. [Online]. Available from: https://flood.gistda.or.th/ [2022 JAN 19].

[30] Notti, D., Giordan, D., Caló, F., Pepe, A., Zucca, F., & Galve, J. P. (2018). Potential and limitations of open satellite data for flood mapping. *Remote sensing*, 10(11), 1673. https://doi.org/10.3390/rs10111673

[31] Craciunescu, V., Stancalie, G., Irimescu, A., Catana, S., Mihailescu, D., Morcov, G., & Constantinescu, S. (2016). MODIS-based multi-parametric platform for mapping of flood affected areas. Case study: 2006 Danube extreme flood in Romania. *Journal of Hydrology and Hydromechanics*, 64(4), 329. https://doi.org/10.1515/johh-2016-0040

[32] Li, S., Sun, D., Goldberg, M. D., Sjoberg, B., Santek, D., Hoffman, J. P., ... & Holloway, E. (2018). Automatic near real-time flood detection using Suomi-NPP/VIIRS data. *Remote sensing of environment*, 204, 672-689. https://doi.org/10.1016/j.rse.2017.09.032

[33] Hardanto, A., Röll, A., Niu, F., Meijide, A., & Hölscher, D. (2017). Oil palm and rubber tree water use patterns: effects of topography and flooding. *Frontiers in plant science*, 8, 452. https://doi.org/10.3389/fpls.2017.00452

[34] Muhadi, N. A., Abdullah, A. F., & Vojinovic, Z. (2017). Estimating agricultural losses using flood modeling for rural area. *In MATEC web of conferences* (Vol. 103, p. 04009). EDP Sciences. https://doi.org/10.1051/matecconf/201710304009

[35] Sumarga, E., Hein, L., Hooijer, A., & Vernimmen, R. (2016). Hydrological and economic effects of oil palm cultivation in Indonesian peatlands. *Ecology and Society*, 21(2). https://doi.org/10.5751/es-08490-210252

[36] Hosseini, F. S., Sigaroodi, S. K., Salajegheh, A., Moghaddamnia, A., & Choubin, B. (2021). Towards a flood vulnerability assessment of watershed using integration of decision-making trial and evaluation laboratory, analytical network process, and fuzzy theories. *Environmental Science and Pollution Research*, 28(44), 62487-62498. https://doi.org/10.21203/rs.3.rs-276992/v1

[37] Rafiei-Sardooi, E., Azareh, A., Choubin, B., Mosavi, A. H., & Clague, J. J. (2021). Evaluating urban flood risk using hybrid method of TOPSIS and machine learning. *International Journal of Disaster Risk Reduction*, 66, 102614. https://doi.org/10.1016/j.ijdrr.2021.102614

[38] Mosavi, A., Golshan, M., Janizadeh, S., Choubin, B., Melesse, A. M., & Dineva, A. A. (2022). Ensemble models of GLM, FDA, MARS, and RF for flood and erosion susceptibility mapping: a priority assessment of sub-basins. *Geocarto International*, 37(9), 2541-2560. https://doi.org/10.1080/10106049.2020.1829101

[39] Azareh, A., Rafiei Sardooi, E., Choubin, B., Barkhori, S., Shahdadi, A., Adamowski, J., & Shamshirband, S. (2021). Incorporating multi-criteria decision-making and fuzzy-value functions for flood susceptibility assessment. *Geocarto International*, 36(20), 2345-2365. https://doi.org/10.1080/10106049.2019.1695958

[40] Taromideh, F., Fazloula, R., Choubin, B., Emadi, A., & Berndtsson, R. (2022). Urban Flood-Risk Assessment: Integration of Decision-Making and Machine Learning. *Sustainability*, 14(8), 4483. https://doi.org/10.20944/preprints202201.0133.v2

[41] Hosseini, F. S., Choubin, B., Mosavi, A., Nabipour, N., Shamshirband, S., Darabi, H., & Haghighi, A. T. (2020). Flash-flood hazard assessment using ensembles and Bayesian-based machine learning models: application of the simulated annealing feature selection method. *Science of the total environment*, 711, 135161. https://doi.org/10.1016/j.scitotenv.2019.135161

[42] Dodangeh, E., Choubin, B., Eigdir, A. N., Nabipour, N., Panahi, M., Shamshirband, S., & Mosavi, A. (2020). Integrated machine learning methods with resampling algorithms for flood susceptibility prediction. *Science of the Total Environment*, 705, 135983. https://doi.org/10.1016/j.scitotenv.2019.135983

[43] Choubin, B., Moradi, E., Golshan, M., Adamowski, J., Sajedi-Hosseini, F., & Mosavi, A. (2019). An ensemble prediction of flood susceptibility using multivariate discriminant analysis, classification and regression trees, and support vector machines. *Science of the Total Environment*, 651, 2087-2096. https://doi.org/10.1016/j.scitotenv.2018.10.064

8 Authors

Supattra Puttinaovarat is an associate professor at the Faculty of Science and Industrial Technology, Prince of Songkla University, Surat Thani Campus. Her research interest includes Geographic Information System, Remote Sensing, Machine Learning, and Information Technology.

Aekarat Saeliw is a lecturer at Faculty of Science and Industrial Technology, Prince of Songkla University, Surat Thani Campus. His research interest includes Information Technology and Mobile Application.

Siwipa Pruitikanee is a lecturer at the Faculty of Science and Industrial Technology, Prince of Songkla University, Surat Thani Campus. Her research interest includes Information Technology and Mobile Application.

Jinda Kongcharoen is an assistant professor at the Faculty of Science and Industrial Technology, Prince of Songkla University, Surat Thani Campus. Her research interest includes Statistics, Applied Statistics, and Information Technology.

Supaporn Chai-Arayalert is an assistant professor at the Faculty of Science and Industrial Technology at Prince of Songkla University, Surat Thani Campus. Her research interests include knowledge management, Green IT, IT project management, e-commerce, and business information systems.

Kanit Khaimook is an associate professor at Ramkhamhaeng University, Bangkok, Thailand. His research interest includes Information Technology and Statistics.

Article submitted 2022-07-28. Resubmitted 2022-09-27. Final acceptance 2022-09-27. Final version published as submitted by the authors.